

Article

Crude Glycerol as an Innovative Corrosion Inhibitor

Isam Al Zubaidi *, Robert Jones, Mohammed Alzughaihi, Moayed Albayyadhi, Farzad Darzi and Hussameldin Ibrahim * 

Industrial Systems Engineering, Faculty of Engineering and Applied Science, University of Regina, 3737 Wascana Parkway, Regina, SK S4S 0A2, Canada; Robert.Jones@uregina.ca (R.J.); mo.yz@hotmail.com (M.Alz.); moayad-1992@windowslive.com (M.Alb.); farzod.darzi@gmail.com (F.D.)

* Correspondence: isam.al.zubaidi@uregina.ca (I.A.Z.); hussameldin.ibrahim@uregina.ca (H.I.); Tel.: 1-306-337-3126 (I.A.Z.); 1-306-337-3347 (H.I.)

Received: 12 February 2018; Accepted: 25 April 2018; Published: 29 April 2018



Abstract: Crude glycerol, a byproduct of biodiesel production, was evaluated as a potential green inhibitor for steel corrosion in an acidic environment. The study was conducted using steel specimens placed in hydrochloric acid solutions (0.5 M) at a constant room temperature (25 °C) and crude glycerol concentrations in the range 0.1%–1.0% w/w. The criteria used to evaluate the extent of corrosion were the weight loss and corrosion rate. Additionally, fresh and spent samples were characterized using scanning electron microscopy and potentiodynamic polarization measurements. It was found that, generally, the corrosion inhibition increased with the inhibitor concentration. Results also showed that the maximum inhibition efficiency was achieved at 70 h residence time after which the inhibition efficiency at a given concentration either remained unchanged or dropped slight. Additionally, the overall maximum inhibition efficiency (98%) was observed at 70 h residence time and a 1% inhibitor concentration.

Keywords: green inhibitor; corrosion; crude glycerol; adsorption isotherms; acidic medium

1. Introduction

Corrosion is the surface decay of metals and non-metallic materials, including ceramics, plastics, rubber, and wood, due to exposure to certain combinations of liquids and/or gases. The mechanism and the rate of corrosion depend on the exact nature of the atmosphere in which the corrosion takes place. Metal corrosion includes the rusting of iron, the tarnishing of silver, the dissolution of metals in acid solutions, and the growth of patina on copper. Corrosion occurs in public infrastructures such as bridges, pipelines, vehicles, utilities (electrical, water, telecommunications, and nuclear power plant), engineering and manufacturing, chemical industry, and the oil and gas industry. Acid solutions are widely used in process industries as corrosion inhibitors through the prevention of metallic scales deposition. The application of corrosion inhibitors has been widely used as an acceptable engineering practice owing to their protective nature against acid attack [1]. Hydrochloric acid (HCl) is widely used for the pickling, cleaning, descaling, and etching of metals [2]. However, HCl is known to be responsible for metal surface corrosion through acid attack mechanisms, resulting in millions of dollars being spent annually on maintenance. It is reported that, with proper corrosion prevention techniques, 25–30% of maintenance costs can be avoided [3]. Applying corrosion inhibitors, even in the smallest amounts, is one of the most economical and environmentally friendly solutions to the metallic corrosion problem [4–10]. Several factors are considered when making a selection of a suitable corrosion inhibitor. This includes cost, effectiveness and the amount to be used, availability and stability, toxicity, and environmental impact. It was found that a number of organic corrosion inhibitors could be used during acid pickling with appreciable inhibition capabilities [11–13]. For example, a mixture of benzotriazole, chitosan, polyacrylic acid, and zinc salt was used as a corrosion and scale inhibitor of carbon steel in

cooling towers [14]. As this organic corrosion and scale inhibitor is phosphate-free, it tends not to cause eutrophication. Considering the product performance and environmental influence, the phosphate-free corrosion and scale inhibitor are superior to the traditional one. Additionally, the application of natural *Jatropha curcas* oil as a steel anti-corrosion agent was recently investigated in a hydrochloric acid medium using weight loss technique, an electrochemical and electrochemical impedance spectroscopy (EIS) polarization technique [15]. It was observed that the corrosion inhibition efficiency increased with inhibitor concentration. Additionally, the potentiodynamic polarization technique revealed that the presence of the natural *Jatropha curcas* oil did not alter the mechanism of hydrogen evolution reaction and instead acted as a surface protection inhibitor. The corrosion inhibition data was fitted to the Frumkin adsorption isotherm model. Hydrazine carbodithioic acid derivatives were also studied as a corrosion inhibitor for mild steel in 0.5 M hydrochloric acid solutions [16]. Langmuir isotherms were used to fit these inhibition adsorption data with adequate accuracy. However, the common denominator for the most widely used corrosion inhibitors is their toxicity and negative environmental impact. Replacing toxic inhibitors with more eco-friendly inhibitors for metal protection in acidic media has been the focus of many studies in recent years. Molasses and vegetable oil have been used as corrosion inhibitors for steel sheets in acid pickling processes [17]. More recently, several studies have focused on the inhibition effect of different environmental friendly materials as corrosion inhibitors for stainless steel and mild steel corrosion in HCl media [18–24]. While organic corrosion inhibitors are toxic in nature, green inhibitors are biodegradable, and contain no heavy metals or other toxic compounds [25]. Spent organic and inorganic inhibitors are released into the environment as aqueous wastes which causes harmful effects to living organisms. In offshore operations, corrosion inhibitors are used to form a barrier layer between the oil and the water phase. The water–inhibitor system is eventually released into the sea, which has toxic effects on marine life [26].

The increasing emphasis on renewable energy is due to the rapid increase in demand for clean transportation fuels, environmental concerns, and shrinking oil reserves. Biodiesel is a biodegradable and renewable fuel that has recently been viewed with increasing interest. Although global biodiesel production was once expected to reach higher levels, the high production cost and the production of high volumes of crude glycerol, a by-product of the biodiesel making, have slowed the rate of biodiesel production [27]. For every 100 kg of biodiesel produced, approximately 10 kg of crude glycerol is generated [28,29]. Crude glycerol is typically transformed to pure glycerol using energy-intensive and expensive processes for applications in the food, pharmaceutical, and cosmetics industries. Various methods for conversion and utilization of crude glycerol have been proposed such as combustion, composting, anaerobic digestion, animal feeds, and thermochemical/biological conversions to value-added products. The chemical composition of crude glycerol depends on the composition of the feedstock, the type of catalyst used in the biodiesel production process, the trans-esterification efficiency, the recovery efficiency of biodiesel, and whether the methanol and catalysts were recovered [30]. Disposal of crude glycerol, which contains salt, methanol, free fatty acids, residual catalyst, etc., represents an economic and environmental challenge. The high cost of purification and market saturation behooves biodiesel producers to seek cheaper and alternate ways to utilize crude glycerol [31]. The presence of impurities has a negative effect on the fermentation process by inhibiting product formation. Hence, microbial fermentation is an alternative and competitive approach for biodiesel producers. Canada's annual biodiesel production in 2018 is estimated at 750 million liters [32]. Hence, large quantities of crude glycerol (~75 million liters) will need to be either purified for use in secondary industries or use in nonconventional applications. In this study, non-purified crude glycerol from biodiesel production was evaluated as a potential green inhibitor for steel specimens in a hydrochloric acid medium.

2. Materials and Methods

2.1. Materials

Steel Specimens

Cylindrically shaped steel specimens of ASTM A6-13A were prepared such that samples will have a length of 22.3 mm, an outside diameter of 9.4 mm, and a side hole diameter of 3.1 mm. The specimens' mechanical properties and chemical compositions are listed in Tables 1 and 2, respectively.

Table 1. Mechanical properties of steel ASTM A6-13A specimens.

Ultimate Tensile (kpsi)	Yield Strength (kpsi)	Elongation (%)
72.105	49.870	21.00

Table 2. Chemical composition of steel ASTM A6-13A specimen in (%) by weight.

C	Mn	P	S	Si	Cu	Ni	Cr	Mo	N	Pb	Sn
0.17	0.67	0.012	0.029	0.18	0.24	0.11	0.04	0.030	0.009	0.004	0.012

The steel specimen was carefully polished with sandpaper of type 9X11 silicon carbide wet-dry 1200 grit, washed thoroughly with tap and distilled water, cleaned from any greasing materials by heptane, washed with distilled water, and cleaned with acetone followed by washing with distilled water. The sample was wiped with clean soft tissues and dried completely by an electric dryer. The crude glycerol sample, used as received, was obtained from one of the biodiesel makers in Saskatchewan, Canada. The physical properties of crude glycerol are shown in Table 3. Specific gravity was measured according to the standard testing method ASTM D1298; pH was measured by dissolving 1 g of crude glycerol in 50 mL of deionized water using a digital pH meter (Oakton Benchtop pH 700 Meter) at controlled room temperature (25 °C). The viscosity of crude glycerol was measured at 25 °C according to ASTM D445 using an Ostwald viscometer. The salt content was measured according to an ASTM D3230 standard method. The 0.5 molar (0.5 M) hydrochloric acid solution was prepared by diluting analytical grade 37% HCl using distilled water, and the resulting solution was kept in a clean glass bottle.

Table 3. Physical properties of crude glycerol.

Property	
Color	Homogeneous dark brownish color
Density, g/mL at 20 °C	1.046
Glycerin content, wt % by mass [33]	80–85
Matter Organic Non Glycerin, % by mass [33]	<2
Salt, % by mass	<7
pH value	11.0
Viscosity, centipoise	286.32

2.2. Experimental Procedure

The dimensions of a specimen were verified using a Vernier caliper and weighted using a high-accuracy (4 significant figures) digital balance. In a typical run, a steel specimen with precisely measured mass and dimensions was hung on an inert material and then immersed in a 0.5 M HCl solution multiple times. For each run, the specimen was cleaned, dried, and weighed precisely.

The steel corrosion rate was determined by measuring weight loss as a function of time. The corrosion rate of mild steel was determined using the relation [34]

$$W = \frac{\Delta m}{S \times t} \quad (1)$$

where Δm is the sample mass loss (g), S the surface area of the specimen (m^2), and t the immersion duration (h). The gravimetric analysis is used in this study to quantify the corrosion extent as described elsewhere [34–36]. The simplicity and reliability of the measurement offered by the weight in this method are such that the technique forms the baseline method of measurement in many corrosion-monitoring programmes. Additionally, the specimens were examined using scanning electron microscopy and Potentiostat measurement.

3. Results and Discussion

3.1. Corrosion Study

This study was performed at a constant and controlled room temperature. Generally, Figure 1a–c show the decrease in the mass of the steel specimen with time. The weight loss of the specimen was gradual but insignificant up to about a 12 h contact time in the acid medium, and the rate of weight loss increased substantially up to 141 h. This means that the mass loss of 0.153% of the original mass of the specimen was observed after 12 h of immersion time in the acid medium and then reached 2.750% by 141 h of contact time. The small weight loss at the beginning of immersion is due to the presence of an oxidation layer on the surface of the specimen, as it requires a longer period of time to be completely removed after a dramatic weight loss up to 141 h. Figure 1a shows the specimen weight loss as a function of immersion time in the HCl solution. Insignificant weight loss (8% loss in specimen weight) was observed up to 35 h of immersion time, and the bulk of weight loss (92% of original mass loss) was observed from 35 to 140 h. Figure 1b shows the % mass loss as a function of residence time. The lower percent mass loss observed initially could be attributed to the remnant oxidation layer on the surface of the steel specimen after polishing and chemical cleaning. The mass loss was then increased rapidly due to the breakage of this layer and the surface of the specimen was in contact directly with the acid material. Figure 1c shows the steel specimen corrosion rate as a function of immersion time in acidic HCl media. The fastest rate of corrosion was observed in the first 12 h of immersion time, and insignificant corrosion rate was observed thereafter. This can be attributed to the formation of an oxidized layer, which was confirmed by SEM analysis performed on the surface of the specimen.

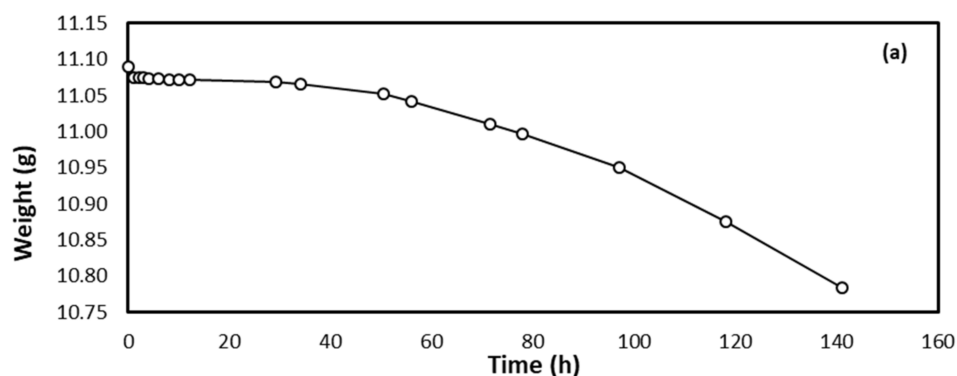


Figure 1. Cont.

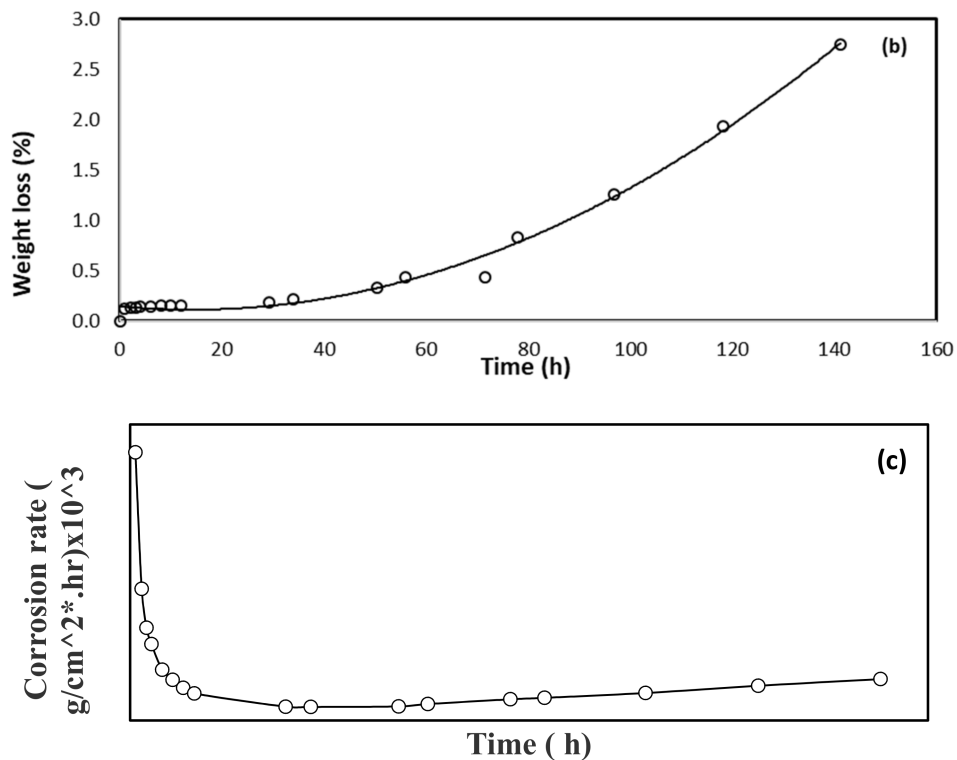


Figure 1. Steel specimen interaction as a function of time in 0.5 M HCl in terms of (a) weight loss in grams, (b) percentage weight loss, and (c) corrosion rate.

3.2. Crude Glycerol Inhibition Ability

Crude glycerol was used as received without any further treatment and mixed with pre-specific amounts of 0.5 M HCl solutions. Different concentrations of glycerol/acid solution were prepared: 0.1%, 0.3%, 0.5%, 0.8%, and 1% by weight. The corrosion inhibition efficiency and the inhibition surface coverage were determined. Figure 2 illustrates the inhibition efficiency (IE %) as a function of immersion time for all inhibitor concentrations. At any given time, the inhibition efficiency increased with the concentration of inhibitor added to the mix. This can be attributed to the formation of a protective glycerol layer on the surface of the steel specimens. For all concentrations, it was observed that maximum inhibition efficiency was achieved at 70 h of residence time, beyond which the efficiency at a given concentration either remained unchanged or dropped slightly. Additionally, the overall maximum inhibition efficiency (98%) was observed at 70 h residence time and 1% inhibitor concentration. This latter value remained unchanged until the experiment was stopped after 120 h.

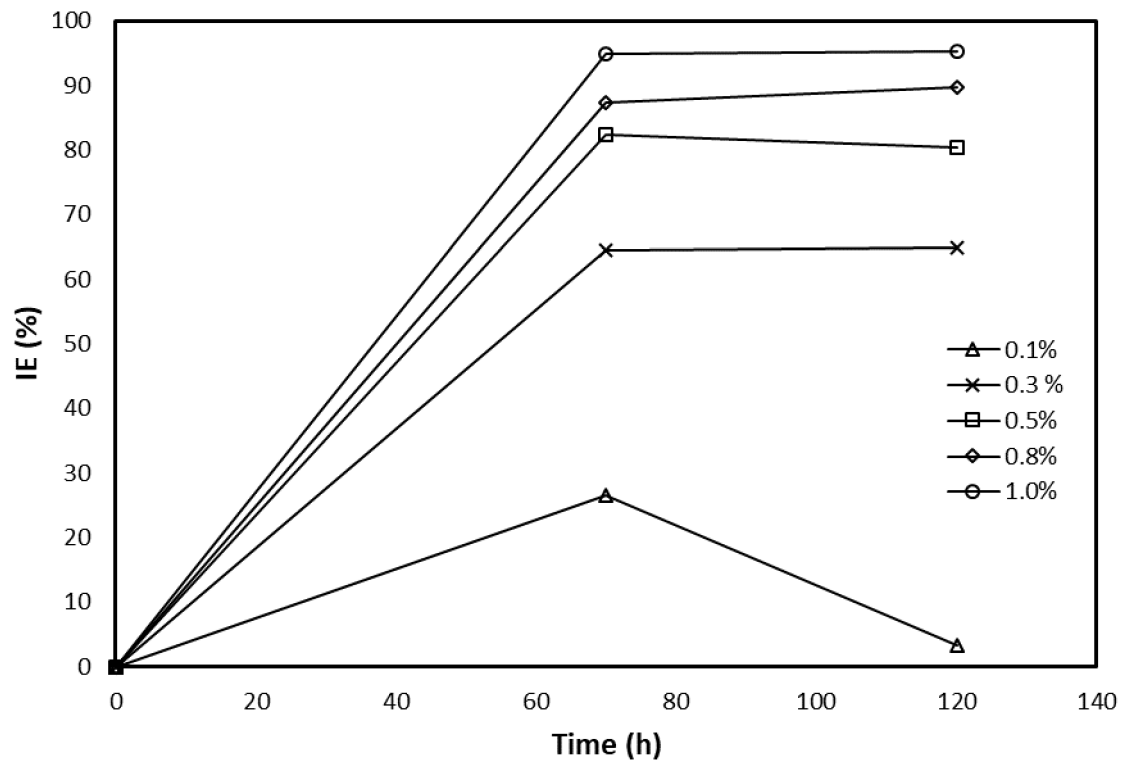


Figure 2. Inhibition efficiency of various glycerol concentrations as a function of immersion time.

Inhibition efficiency (IE %) and the degree of surface coverage (θ) of the glycerol inhibitor for the corrosion study of steel in 0.5 M HCl were calculated using Equation (2) [35–39]:

$$IE \% = \theta \times 100 = [(W_0 - W) / W_0] \times 100 \tag{2}$$

where W_0 and W are the average weight losses in the absence and presence of the crude glycerol inhibitor, respectively. The inhibition efficiency increased with an increase in crude glycerol concentration. The primary action of inhibitors in acid solution is believed to be adsorption on the metal surface. This involves the assumption that the corrosion reactions are prevented from occurring over the active sites of the metal surface covered by adsorbed inhibitor species and the corrosion reaction occurred mainly on the inhibitor-free sites [40,41]. In this work, the concentration of the crude glycerol was kept below 1% due to the basic nature of crude glycerol, which may reduce the performance of the acid solution in the studied system. The fraction of a covered surface (θ) is determined as a function of concentration at specific constant temperature, and the adsorption isotherm was subsequently evaluated at equilibrium condition. The concentration C is plotted against the surface coverage as shown in Figure 3. As expected, the surface coverage increased with concentration.

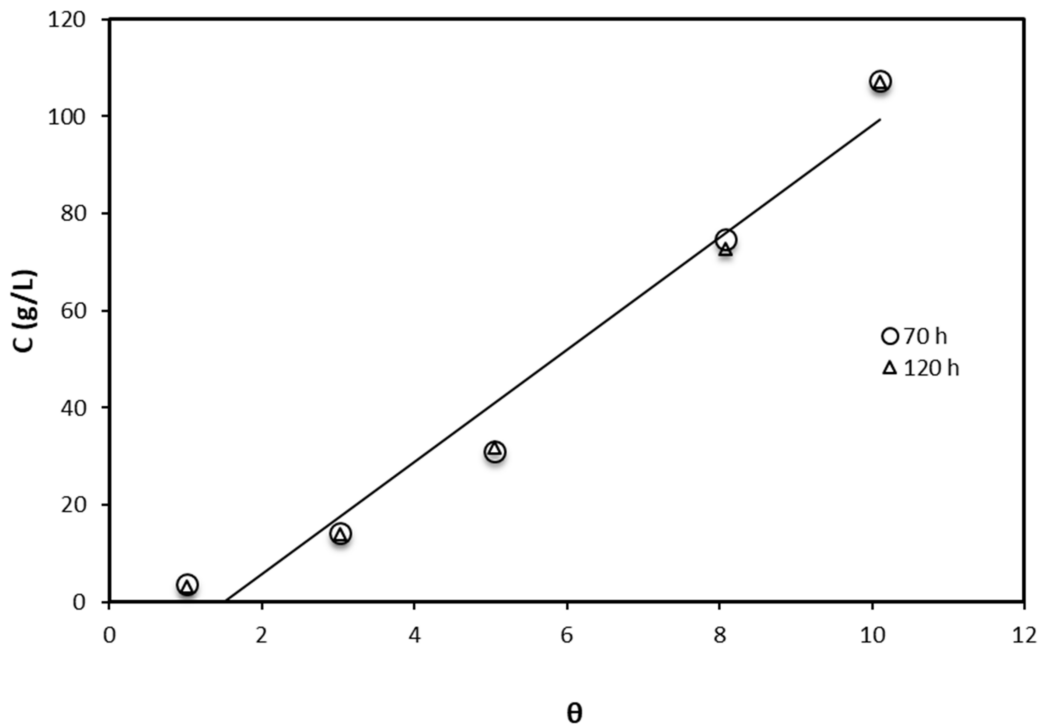


Figure 3. Concentration as a function of surface coverage for the inhibition effect of crude glycerol.

The three most common adsorption isotherms, namely the Langmuir, Freundlich, and Temkin isotherms, were tested to fit the data and adequately describe the process in this study. The Langmuir isotherm suggested the dependence of the fraction of the surface covered θ on the concentration of the inhibitor C according to Equation (3):

$$C_e/q_e = 1/k_l q_m + C_e/q_m \tag{3}$$

where C_e is the equilibrium inhibitor concentration, k_l the Langmuir equilibrium constant, representing the degree of adsorption (i.e., the higher the value of k_l indicates that the inhibitor is strongly adsorbed on the metal surface). The Langmuir isotherm plot of C_e/q_e versus C_e is a straight line with positive slopes, as shown in Figure 4.

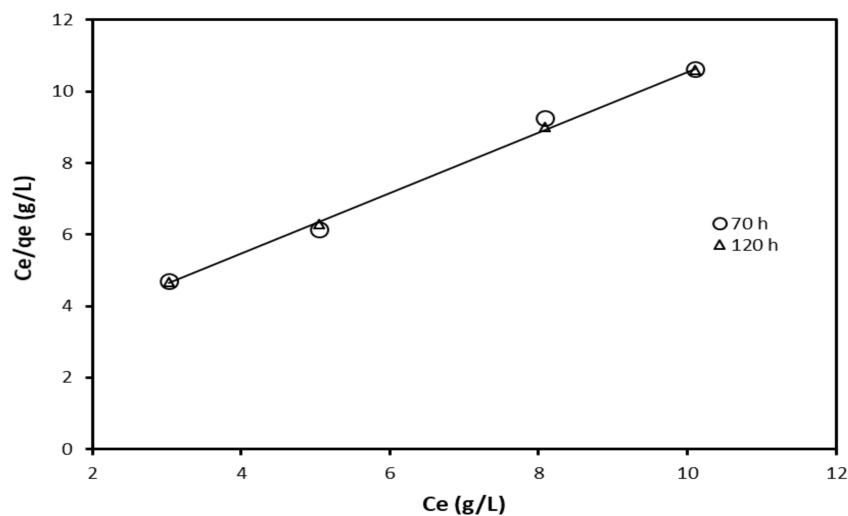


Figure 4. Langmuir adsorption isotherm for the inhibition effect of crude glycerol.

The experimental data were fitted to Langmuir adsorption isotherm model, and the results are presented in Figure 4. The model was then used to predict the adsorption constant. The adsorptive equilibrium constant was estimated to be 0.483 and 0.5077 g/L after 70 and 120 h, respectively. The deviation from unity slope indicates that the Langmuir isotherm may not be strictly applied in this case. Hence, other adsorption isotherms need to be tested.

The experimental results were also fitted to a Freundlich adsorption isotherm. The Freundlich adsorption isotherm is given according to Equation (4):

$$\log q_e = \log k_f + 1/n \log C_e \tag{4}$$

where k_f and n are Freundlich constants; q_e = amount of adsorbent per unit mass of adsorbate (g/g); C_e = equilibrium concentration (mg/L). The $\log q_e$ versus $\log C_e$ plot allows for a determination of the Freundlich constants. The results of adsorption isotherm models are shown in Figure 5.

According to Equation (4), when $\log q_e$ is plotted against $\log C_e$, it gives a straight line with intercept ($\log k_f$) and slope ($1/n$), as can be observed from Figure 5.

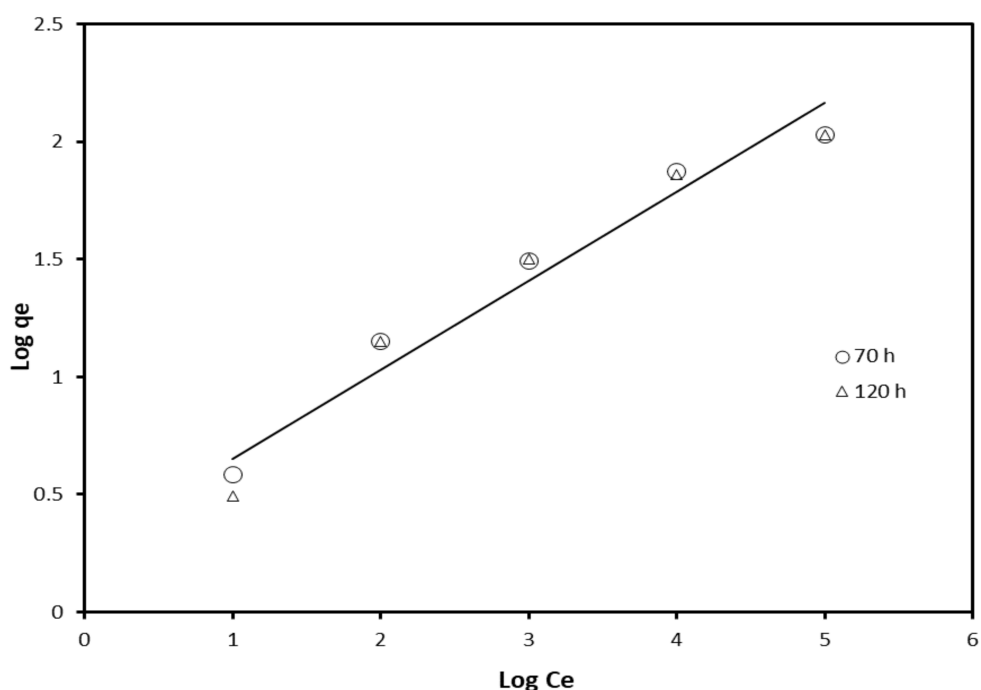


Figure 5. Freundlich adsorption isotherm for the inhibition effect of crude glycerol.

The values of $n = 0.362$ for inhibition after 70 h and 0.378 after 120 h of inhibition.

The Temkin adsorption isotherm was also applied by plotting q_e versus $\ln C_e$ after 70 and 120 h. According to the Temkin isotherm model (Equation (5)), the plot of surface coverage (q_e) obtained from the weight loss method versus $\ln C_e$ at different concentrations of the inhibitors is not a straight line as shown in Figure 6.

$$q_e/B = \ln A + \ln C_e \tag{5}$$

where $B = (RT/b)$ constant related to heat of sorption (J/mol) obtained from the Temkin plot (q_e versus $\ln C_e$); A (intercept) = Temkin isotherm equilibrium binding constant; b (slope) = Temkin isotherm constant; R = universal gas constant; T = absolute temperature.

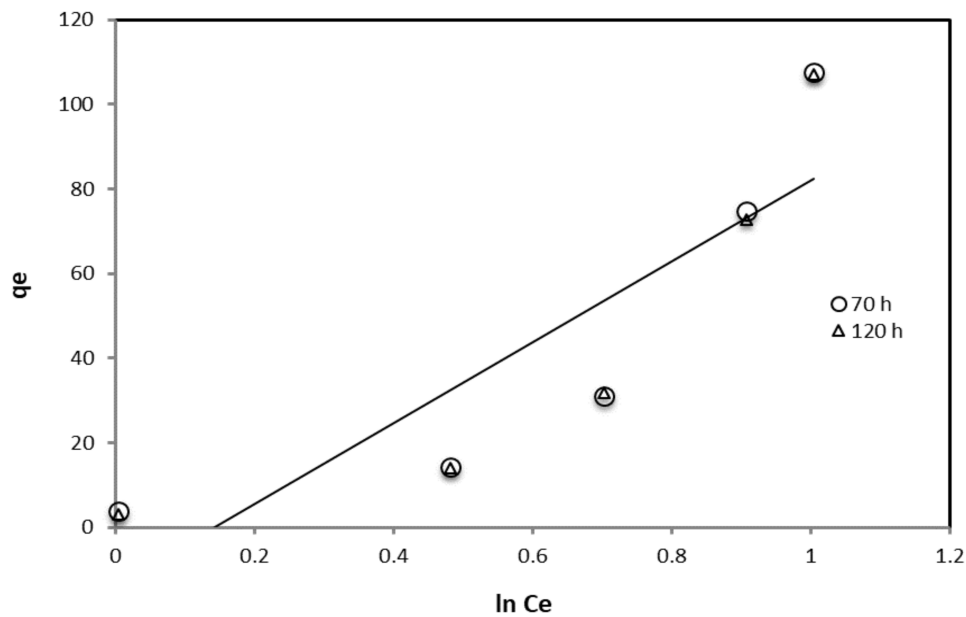


Figure 6. The Temkin adsorption isotherm for the inhibition effect of crude glycerol.

A summary of the adsorption isotherm models is given in Table 4.

Table 4. Summary of the adsorption isotherm models for the inhibition of crude glycerol.

Adsorption Isotherm Model	Contact Time (h)	R ²	K _{ad} , g/L, Slope	Intercept
Langmuir	70	0.999	0.848	2.069
	120	0.994	0.869	1.970
Freundlich	70	0.965	0.362	0.342
	120	0.952	0.378	0.273
Temkin	70	0.853	0.0085	0.1848
	120	0.8532	0.0085	0.1859

From the table, it can be concluded that the corrosion inhibition using crude glycerol is best-described using Langmuir adsorption isotherm compared to the other two models. In this study, the corrosion of steel in 0.5 M HCl, the weight at time t denoted as W_1 when $\log W_1$ is plotted versus time, a linear correlation is observed as given by Figure 7. This suggests first-order reaction kinetics.

$$\log W_1 = \log W_0 - K t \tag{6}$$

where W_0 is the weight before immersion, K is the rate constant, and t is the time in h.

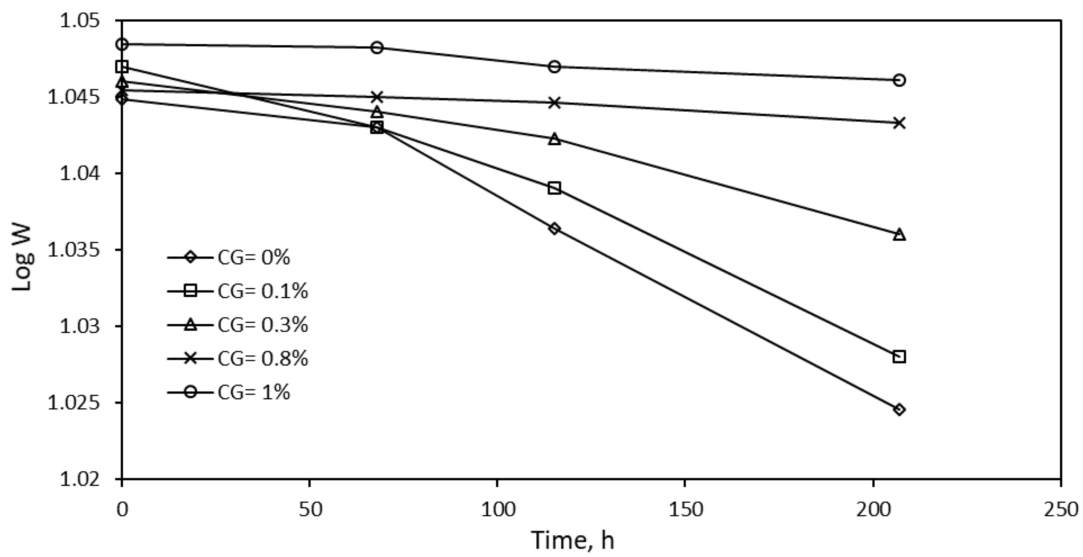


Figure 7. Effect of immersion time on specimen weight at a given time.

The value of the rate constant K is obtained from the slope of the straight line. The half-life value, $t_{1/2}$ of the metal in the test solution, can be determined using Equation (7) [42–44]:

$$t_{1/2} = \frac{0.693}{K} \tag{7}$$

The equilibrium constant of the adsorption process is related to the Gibbs free energy of adsorption ΔG_{ads} as shown in Equation (8) [44].

$$\Delta G = -2.303RT \log(55.5 K) \tag{8}$$

here R is the gas constant, T is the absolute temperature, and K is the adsorption equilibrium constant. The values of K were obtained using Equation (9) [45].

$$K = \frac{\theta}{[(1 - \theta)C]} \tag{9}$$

where C is the concentration of the extract, usually for the adsorption of free energy involved in a physical process, $\Delta G_{ads} < -40$ kJ/mol [42]. The negative value of ΔG_{ads} suggests that the adsorption of crude glycerol onto the metal surface is a spontaneous process and the adsorbed layer is stable. The values of R^2 , K , $t_{1/2}$, and ΔG_{ads} for the corrosion reaction in the presence and absence of the inhibitor are given in Table 5.

Table 5. Parameters estimation for the corrosion of steel specimen in the absence and in the presence of inhibitor.

	R^2	$K, \times 10^5$	$t_{1/2} (\times 10^{-4}), s$	$\Delta G_{ads}, \text{ kJ/mol}$
0% CG	0.925	1	6.93	-12.741
0.1% CG	0.956	1	6.93	-12.741
0.3% CG	0.953	5	1.386	-14.441
0.8%CG	0.971	9	0.77	-13.000
1.0% CG	0.935	10	0.693	-24.037

Generally, the values of ΔG_{ads} up to -20 kJ/mol are constant with the electrostatic interaction between the charged molecules and charged metal (physisorption), while the negative values higher

than -40 kJ/mol involve sharing or transfer of electrons from the inhibitors to the metal surface to form a coordinate type of bond (chemisorption) [41]. The crude glycerol molecules may arrange themselves on the metal surface such that it becomes difficult for the surface to adsorb further molecules from neighboring sites. This suggests that a multilayer-adsorption mechanism may take place. The net result is the formation of various surface sites with varying degrees of activity.

3.3. Scanning Electron Microscopy (SEM)

Scanning electron microscopy (SEM) images for the surfaces of fresh and corroded steel specimens were collected using a JSM5600 (JEOL, Tokyo, Japan). This study was performed to determine the surface morphology of the steel specimen. For each sample, images were collected at $2000\times$ magnification. SEM images of a fresh steel specimen, a steel specimen after corrosion using a 0.5 M HCl medium, and a specimen after corrosion inhibition with different concentrations of crude glycerol were taken to investigate the metal surface changes after three days of residence time in hydrochloric acid solutions with different concentrations of crude glycerol. Figure 8 shows the SEM images of the different tested scenarios. As can be seen from the SEM images, the steel surface is severely damaged and altered due to an aggressive attack of the corroding medium. Figure 8c shows that the corrosion marks on the surface of the metal decrease in the presence of crude glycerol. This suggests that the crude glycerol has the ability to adsorb on the surface of the steel specimen exhibiting greater protection towards steel corrosion. The protective crude glycerol layer becomes thicker as the concentration of inhibitor is increased. The parallel lines on the carbon steel surface can be attributed to polishing scratches.

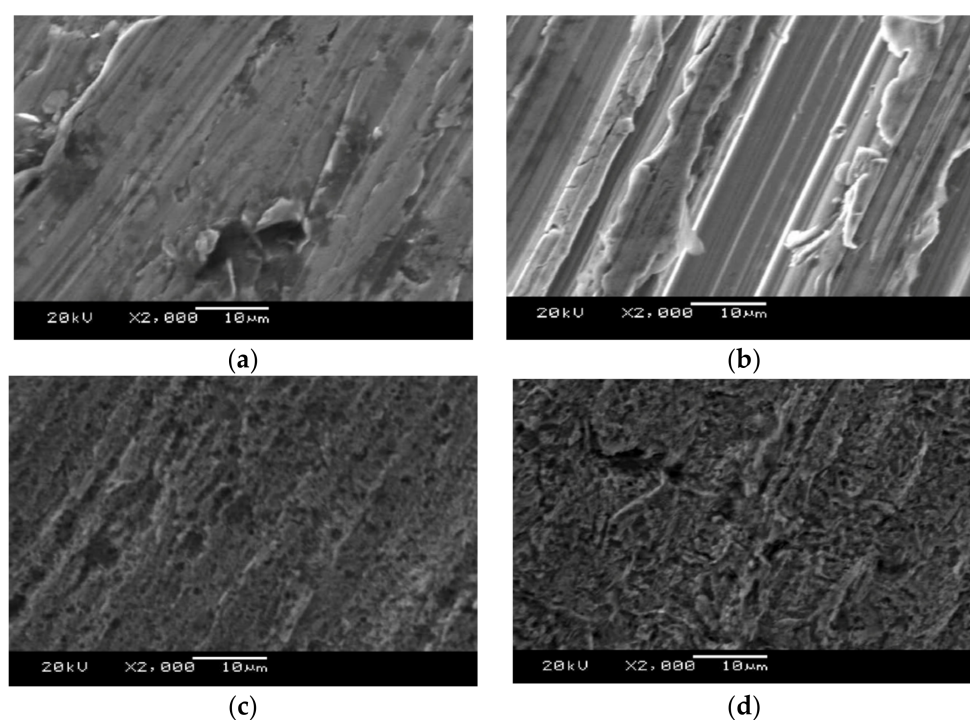


Figure 8. SEM images of (a) a new steel specimen, (b) the corrosion of a steel specimen with 0.5 M HCl, (c) a steel specimen after corrosion inhibition with 0.3 wt % waste glycerol, and (d) a steel specimen after corrosion inhibition with 0.5 wt % waste glycerol.

3.4. Potentiodynamic Polarization Measurements

The Potentiostat samples for electrochemical experiments were machined into test electrodes of dimension 1×1 cm and fixed in polytetrafluoroethylene (PTFE) rods by epoxy resin in such a way

that only one surface, with an area of 1 cm², was left uncovered. The exposed surface was cleaned. Electrochemical experiments were conducted in a conventional three-electrode glass cell of 400 mL using a complete DC voltammetry and corrosion system. A graphite rod was used as a counter electrode and a saturated calomel electrode (SCE) as a reference electrode.

The effect of crude glycerol concentration in the polarization curves for steel specimens in 0.5 M HCl is shown in Figure 9. This curve represents the anodic and cathodic polarization curves of the steel specimens. Both anodic and cathodic polarization curves are shifted to lower current density values in the presence of crude glycerol. This behavior suggests the inhibitive action of the inhibitor. The extent of the shift in current density increases with increasing glycerol concentrations. The values of corrosion current density (*i*_{corr}), corrosion potential (*E*_{corr}), anodic Tafel constants (β_a), and cathodic Tafel constant (β_c), excluded from polarization curves are given in Table 6.

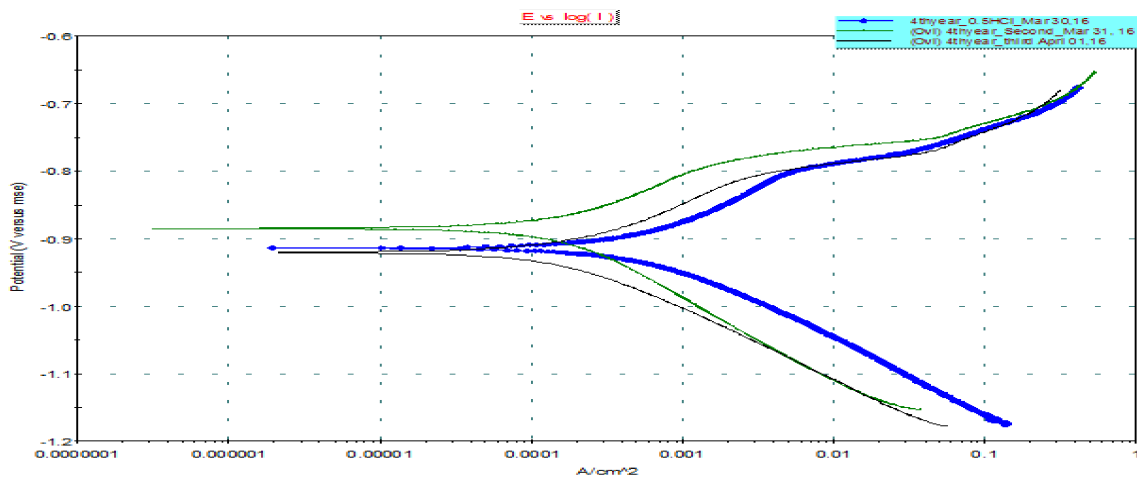


Figure 9. E versus log I for steel in 0.5 M HCl without and with inhibitor. Corrosion rate (mpy) of 0.5 M HCl solution = 56.6; corrosion rate (mpy) of 0.5 M HCl + crude glycerol (0.1%) = 16.9; corrosion rate of (mpy) of 0.5 M HCl + crude glycerol (0.8%) = 19.97.

Table 6. Tafel fit minimizing x error (no inhibitor).

	Without Inhibition	With Inhibition
E (I = 0) (mV):	−914.082	−884.460
I _{corr} (μA):	602.7	212.5
Ca. Beta (mV):	108.714	149.183
An. Beta (mV):	120.478	108.848
Co. Rate (mpy):	56.66	19.97
Chi-Square:	0.58	5.96
Fit Range (mV):	(−1005), (−811)	(−1021), (−785)
Fit Mode:	Auto	Auto

Table 6 reveals that the corrosion potential of steel specimens in the acid solution is largely shifted to more negative values (the noble direction) upon the addition of crude glycerol. On the other hand, the corrosion current density is greatly reduced upon the addition of the inhibitor. These results suggest the inhibitive effects of the crude glycerol. The data in Table 6 reveal that the values of inhibition efficiency obtained by polarization are comparable to those obtained by weight loss measurements. The inhibition efficiency increases with increasing inhibitor concentration. The addition of increasing concentrations of crude glycerol decreases both the anodic and cathodic Tafel constants. This result indicates that the inhibitor acts as a mixed inhibitor [42]. This means that the inhibitor molecules are adsorbed on both the anodic and cathodic sites, resulting in the inhibition of both anodic dissolution

and cathodic reduction reactions. As the metal surface area occupied by adsorbed molecules increases, inhibition efficiency increases.

4. Conclusions

On the basis of this study, the following conclusions can be drawn. Crude glycerol from biodiesel production plants can be evaluated as a corrosion inhibitor for ASTM A6-13A steel specimen in 0.5 M HCl solutions. The inhibition effect was increased as concentration of the inhibitor increased. The weight loss technique was in agreement with the potentiodynamic polarization measurements. Many concentrations of crude glycerol were taken in the range of 0.1–1.0%. The highest level of corrosion inhibition was obtained using a 1% inhibitor concentration. The SEM images showed that a thin layer of the inhibitor formed on the specimen surface and acted as a protective layer against corrosion. The corrosion inhibition is probably due to the adsorption (physical and chemical) of the crude glycerol on the metal surface protecting it from acid attack. The inhibition mechanism of crude glycerol followed a Langmuir adsorption isotherm model. Adsorption parameters were also estimated.

Author Contributions: H.I. and I.A.Z. secured funding and proposed the original idea; H.I., I.A.Z., and R.J. provided direction and guidance; M.Alz., M.Alb., and F.D. drafted the manuscript; H.I. and I.A.Z. provided critical revision and wrote sections of the final draft; H.I. and I.A.Z. supervised the project and provided final approval of the version to be published.

Acknowledgments: The authors would like to thank the Industrial Systems Engineering program at the University of Regina for providing the necessary infrastructure to successfully complete this work. Additionally, the support of the Engineering Workshop at the Faculty of Engineering is gratefully acknowledged.

Conflicts of Interest: The authors declare no conflict of interest.

References

1. Khan, G.; Newaz, K.S.; Basirun, W.J.; Ali, H.B.M.; Faraj, F.L.; Khan, G.M. Application of natural product extracts as green corrosion inhibitors for metals and alloys in acid pickling processes—A review. *Int. J. Electrochem. Sci.* **2015**, *10*, 6120–6134.
2. Cardarelli, F. *Materials Handbooks—A Concise Desktop Reference*; Springer: London, UK, 2000.
3. Gerhardus, H.K.; Michiel, P.H.; Bronger, N.G.; Thompson, Y.; Paul, V.; Payer, J.H. *Corrosion Cost and Preventive Strategies in the United States. Supplement to Materials Performance*; Report number FHWA. RD-01-156; Federal Highway Administration: Mclean, VA, USA, 2002.
4. Bouklah, M.; Hammouti, B.; Lagrenée, M.; Bentis, F.M. Thermodynamic properties of 2,5-bis (4-methoxyphenyl)-1,3,4-oxadiazole as a corrosion inhibitor for mild steel in normal sulfuric acid medium. *Corros. Sci.* **2006**, *48*, 2831–2842. [[CrossRef](#)]
5. Raja, P.B.; Sethuraman, M.G. Natural products as corrosion inhibitor for metals in corrosive media—A review. *Mater. Lett.* **2008**, *62*, 113–116. [[CrossRef](#)]
6. Wang, L.; Pu, J.X.; Luo, H.C. Corrosion inhibition of zinc in phosphoric acid solution by 2-mercaptobenzimidazole. *Corros. Sci.* **2003**, *45*, 677–683. [[CrossRef](#)]
7. El-Etre, A.Y. Natural honey as corrosion inhibitor for metals and alloys, Copper in neutral aqueous solution. *Corros. Sci.* **1998**, *40*, 1845–1850. [[CrossRef](#)]
8. Radojic, I.; Berkovic, K.; Kovac, S.; Vorkapic-Furac, J. Natural honey and black radish juice as tin corrosion inhibitors. *Corros. Sci.* **2008**, *50*, 1498–1504. [[CrossRef](#)]
9. Ahmad, Z. *Principles of Corrosion Engineering and Corrosion Control*; Elsevier: Oxford, UK, 2006.
10. Roberge, P.R. *Handbook of Corrosion Engineering*; McGraw-Hill: New York, NY, USA, 2000.
11. Ali, S.A.; Al-Muallem, H.A.; Rahman, S.U.; Saeed, M.T. Bis-isoxazolines: A new class of corrosion inhibitors of mild steel in acidic media. *Corros. Sci.* **2008**, *50*, 3070–3377. [[CrossRef](#)]
12. Mernari, B.; El Attari, H.; Traisnel, M.; Bentiss, F.; Lagrenée, M. Inhibiting effects of 3,5-bis (*n*-pyridyl)-4-amino-1,2,4-triazoles on the corrosion for mild steel in 1 M HCl medium. *Corros. Sci.* **1998**, *40*, 391–399. [[CrossRef](#)]

13. El Achouri, M.; Kertit, S.; Goultaya, H.M.; Nciri, B.; Bensouda, Y.; Perez, L.; Infante, M.R.; Elkacemi, K. Corrosion inhibition of iron in 1 M HCl by some gemini surfactants in the series of alkanediyl- α,ω -bis-(dimethyl tetradecyl ammonium bromide). *Prog. Org. Coat.* **2001**, *43*, 267–273. [[CrossRef](#)]
14. Zeng, D.; Yan, H. Experimental study on a new corrosion and scale inhibitor. *J. Environ. Protect.* **2013**, *4*, 671–675. [[CrossRef](#)]
15. Mokhtari, O.; Hamdani, I.; Chetouani, A.; Lahrach, A.; El Halouani, H.; Aouniti, A.; Berrabah, M. Inhibition of steel corrosion in 1M HCl by Jatropha curcas oil. *J. Mater. Environ. Sci.* **2014**, *5*, 310–319.
16. Khaled, K.F. Experimental and theoretical study for corrosion inhibition of mild steel in hydrochloric acid solution by some new hydrazine carbodithioic acid derivatives. *Appl. Surf. Sci.* **2016**, *252*, 4120–4128. [[CrossRef](#)]
17. Fouda, A.S.; Elewady, G.Y.; Shalabi, K.; Habbouba, S. Gibberellic acid as green corrosion inhibitor for carbon steel in hydrochloric acid solutions. *J. Mater. Environ. Sci.* **2014**, *5*, 767–778.
18. Sangeetha, M.; Rajendran, S.; Muthumegala, T.S.; Krishnaveni, A. Green corrosion inhibitors-An overview. *Zaštita Materijala* **2011**, *52*, 3–19.
19. Fouda, A.S.; Elewady, G.Y.; Shalabi, K.; Habouba, S. Anise extract as green corrosion inhibitor for carbon steel in hydrochloric acid solutions. *Int. J. Innov. Res. Sci.* **2014**, *3*, 11210–11228.
20. Obot, I.B.; Obi-Ebbed, N.O. 2,3-Diphenylbenzoquinoxaline: A new corrosion inhibitor for mild steel in sulphuric acid. *Corros. Sci.* **2010**, *52*, 282–285. [[CrossRef](#)]
21. Obot, I.B.; Obi-Egbedi, N.O.; Odozi, N.W. Acenaphtho [1,2-b] quinoxaline as a novel corrosion inhibitor for mild steel in 0.5 M H₂SO₄. *Corros. Sci.* **2010**, *52*, 923–926. [[CrossRef](#)]
22. Obot, I.B.; Obi-Egbedi, N.O. Indeno-1-one [2, 3-b] quinoxaline as an effective inhibitor for the corrosion of mild steel in 0.5 M H₂SO₄ solution. *Mater. Chem. Phys.* **2010**, *122*, 325–328. [[CrossRef](#)]
23. Kesavan, D.; Gopiraman, M.; Sulochana, N. Green inhibitors for corrosion of metals: A review. *Chem. Sci. Rev. Lett.* **2012**, *1*, 1–8.
24. Yang, F.; Hanna, M.A.; Sun, R. Value-added uses for crude glycerol—A byproduct of biodiesel production. *Biotechnol. Biofuels* **2012**, *5*, 1–10. [[CrossRef](#)] [[PubMed](#)]
25. Neha, P.; Shruti, A.; Pallav, S. Greener Approach towards Corrosion Inhibition. *Chin. J. Eng.* **2013**, *2013*. [[CrossRef](#)]
26. Singh, W.P.; Bockris, J.O. NACE-96225, *Corrosion 96*; NACE International: Denver, CO, USA, 24–29 March 1996.
27. Bewley, B.R.; Berkaliev, A.; Henriksen, H.; Ball, D.B.; Ott, L.S. Waste glycerol from biodiesel synthesis as a component in deep eutectic solvents. *Fuel Process. Technol.* **2015**, *138*, 419–423. [[CrossRef](#)]
28. Johnson, D.T.; Taconi, K.A. The Glycerin Glut: Options for the Value-Added Conversion of Crude Glycerol Resulting from Biodiesel Production. *Environ. Prog.* **2007**, *26*, 338–348. [[CrossRef](#)]
29. Thompson, J.C.; He, B.B. Characterization of Crude Glycerol from Biodiesel Production from Multiple Feedstocks. *Appl. Eng. Agric.* **2006**, *22*, 261–265. [[CrossRef](#)]
30. Hansen, C.F.; Hernandez, A.; Mullan, B.P.; Moore, K.; Trezona-Murray, M.; King, R.H.; Pluske, J.R. A chemical analysis of samples of crude glycerol from the production of biodiesel in Australia, and the effects of feeding crude glycerol to growing-finishing pigs on performance, plasma metabolites and meat quality at slaughter. *Anim. Prod. Sci.* **2009**, *49*, 154–161. [[CrossRef](#)]
31. Chozhavendhan, S.; Praveen Kumar, R.; Elavazhagan, S.; Barathiraja, B.; Jayakumar Sunita, M.; Varjani, J. Utilization of Crude Glycerol from Biodiesel Industry for the Production of Value-Added Bioproducts. In *Waste to Wealth*; Springer Publisher: New York, NY, USA, 2017; pp. 65–82.
32. Darlene, D. *Biofuels Annual 2016*; Gain Report No. CA16038; USD Foreign Agricultural Service: Washington, DC, USA, 2016.
33. Hu, S.; Luo, X.; Wan, C.; Li, Y. Characterization of Crude Glycerol from Biodiesel Plants. *J. Agric. Food Chem.* **2012**, *60*, 5915–5921. [[CrossRef](#)] [[PubMed](#)]
34. Al Zubaidi, I.; Ibrahim, H.; Jones, R.; Al zughaibi, M.; Albayyadhi, M.; Darzi, F. Waste glycerol as new green inhibition for metal corrosion in acid medium. In Proceedings of the 3rd International Conference on Fluid Flow, Heat and Mass Transfer (FFHMT'16), Ottawa, ON, Canada, 2–3 May 2016.
35. Yaro, A.S.; Khadom, A.A.; Wael, R.K. Apricot juice as green corrosion inhibitor of mild steel in phosphoric acid. *Alex. Eng. J.* **2013**, *52*, 129–135. [[CrossRef](#)]
36. Umoren, S.A.; Ebenso, E.E. Studies of the anti-corrosive effect of Raphia hookeri exudate gum-halide mixtures for aluminum corrosion in acidic medium. *Pigment Resin Technol.* **2008**, *37*, 17–23. [[CrossRef](#)]

37. Pujar, M.G.; Anita, T.; Shaikh, H.; Dayal, R.K.; Khatak, H.S. Analysis of electrochemical noise data using MEM for pitting corrosion of 316 SS in Chloride Solution. *Int. J. Electrochem. Sci.* **2007**, *2*, 301–310.
38. Oguzie, E.E. Corrosion inhibition of mild steel in hydrochloric acid solution by methylene blue dye. *Mater. Lett.* **2005**, *59*, 1076–1079. [[CrossRef](#)]
39. Shreir, L.L.; Jarman, R.A.; Burstein, G.T. *Corrosion*, 3rd ed.; Newnes-Butterworths: London, UK, 1994; Volume 2.
40. Umoren, S.A.; Obot, I.B.; Obi-Egbedi, N.O. Raphia hookeri gum as a potential eco-friendly inhibitor for mild steel in sulfuric acid. *J. Mater. Sci.* **2009**, *44*, 274–279. [[CrossRef](#)]
41. Nwosu, O.F.; Osarolube, E.; Nnanna, L.A.; Akoma, C.S.; Chigbu, T. Acidic Corrosion Inhibition of Piper guineense Seed Extract on Al Alloy. *Am. J. Mater. Sci.* **2014**, *4*, 178–183.
42. Sivaraju, P.K.; Arulanantham, A. Inhibitive properties of plant extract (*Acalypha indica* L.) on mild steel corrosion in 1N phosphoric acid. *Int. J. Chem. Technol. Res.* **2010**, *2*, 256–265.
43. de Souza, F.S.; Spinelli, A. Caffeic acid as a green corrosion inhibitor for mild steel. *Corros. Sci.* **2009**, *51*, 642–649. [[CrossRef](#)]
44. Ansari, A.; Znini, M.; Hamdani, I.; Majidi, L.; Bouyanzer, A.; Hammouti, B. Experimental and theoretical investigations anti-corrosive properties of Menthone on mild steel corrosion in hydrochloric acid. *J. Mater. Environ. Sci.* **2014**, *5*, 81–94.
45. El-Awady, A.A.; Abd-El-Nabey, B.A.; Aziz, S.G. Kinetic thermodynamic and adsorption isotherms analyses for the inhibition of the acid corrosion of steel by cyclic and open chain amines. *J. Electrochem. Soc.* **1992**, *139*, 2149–2154. [[CrossRef](#)]



© 2018 by the authors. Licensee MDPI, Basel, Switzerland. This article is an open access article distributed under the terms and conditions of the Creative Commons Attribution (CC BY) license (<http://creativecommons.org/licenses/by/4.0/>).